Published in final edited form as:

Neurobiol Dis. 2020 February ; 134: 104711. doi:10.1016/j.nbd.2019.104711.

Sex may influence motor phenotype in a novel rodent model of cerebral palsy

Bhooma R. Aravamuthan[a,b,c,*], **Sushma Gandham**[a], **Anne B. Young**[c,d], **Seward B. Rutkove**[c,e]

[a]Washington University in St Louis School of Medicine, St Louis, MO, USA

[b]Boston Children's Hospital Boston, MA, USA

[c]Harvard Medical School Boston, MA, USA

[d]Massachusetts General Hospital, Boston, MA, USA

[e]Beth Israel Deaconess Medical Center, Boston, MA, USA

Abstract

Cerebral palsy (CP) is the most common cause of childhood motor disability, manifesting most often as spasticity and/or dystonia. Spasticity and dystonia are often co-morbid clinically following severe injury at term gestation. Currently available animal CP models have not demonstrated or differentiated between these two motor phenotypes, limiting their clinical relevance. We sought to develop an animal CP model displaying objectively identifiable spasticity and dystonia. We exposed rat pups at post-natal day 7–8 (equivalent to human 37 postconceptional weeks) to global hypoxia. Since spasticity and dystonia can be difficult to differentiate from each other in CP, objective electrophysiologic markers of motor phenotypes were assessed. Spasticity was inferred using an electrophysiologic measure of hyperreflexia: soleus Hoffman reflex suppression with 2 Hz tibial nerve stimulation. Dystonia was assessed during voluntary isometric hindlimb withdrawal at different levels of arousal by calculating tibialis anterior and triceps surae electromyographic co-activation as a surrogate of overflow muscle activity. Hypoxia affected spasticity and dystonia measures in a sex-dependent manner. Males had attenuated Hoffman reflex suppression suggestive of spasticity but no change in antagonist muscle co-activation. In contrast, females demonstrated increased co-activation suggestive of dystonia but no change in Hoffman reflex suppression. Therefore, there was an unexpected segregation of electrophysiologically-defined motor phenotypes based on sex with males predominantly demonstrating spasticity and females predominantly demonstrating dystonia. These results require human clinical confirmation but suggest that sex could play a critical role in the motor manifestations of neonatal brain injury.

Keywords

Cerebral palsy; Neonatal brain injury; Dystonia; Spasticity; Animal models of disease

[*]Corresponding author at: Department of Neurology, Division of Pediatric Neurology, Washington University School of Medicine, 660 South Euclid Avenue, Campus Box 8111, St. Louis, MO 63110-1093, USA. aravamuthanb@wustl.edu (B.R. Aravamuthan).

Author roles

B.A., A.B.Y., and S.B.R contributed to the conception and design of the study. B.A. and S.G. contributed to the acquisition and analysis of data. B.A. and S.B.R. contributed to drafting the manuscript and figures.

1. Introduction

Cerebral palsy (CP) is the most common cause of motor disability in childhood (Ashwal et al., 2004; Dressier, 2011; Himmelmann et al., 2009). CP motor phenotypes include spasticity and dystonia, which are often co-morbid. Differentiation between spasticity and dystonia is critical as they require different treatments and often have different functional implications (Fehlings et al., 2018; Lin et al., 2014). Clinical epidemiological studies of CP suffer from having to draw population conclusions from children who have highly variable forms of neonatal brain injury (including prematurity, infection, stroke, and neonatal hypoxic-ischemic injury at term gestation). Studying CP pathophysiology in animal models allows for standardization of neonatal brain injury mechanism and thus may uncover possible risk factors for different motor outcomes that are not readily apparent from population-based clinical studies alone.

A clinically-relevant animal model of CP should display spasticity and dystonia. Dystonia is “initiated or worsened by voluntary action, and associated with overflow muscle activation”(Albanese et al., 2013) and its “magnitude…varies with arousal” (Sanger et al., 2010). Spasticity is increased “resistance to externally imposed movement…with increasing speed of stretch” and is associated with hyperreflexia (Sanger et al., 2010). Notably, the converse is not true (Albanese et al., 2013; Sanger et al., 2010). Spasticity is not preferentially triggered by voluntary movement and varies little with arousal. Dystonia is not associated with hyperreflexia.

Differentiation between dystonia and spasticity in animal models can be difficult (Oleas et al., 2013; Shakkottai et al., 2017). Though clasping or twisting in rodents has been called dystonic, these behaviors are also present in spastic rats (Ryu et al., 2017). Therefore, these behaviors cannot effectively discriminate between dystonia and spasticity. However, electrophysiologic measures of tone could objectively differentiate between dystonia and spasticity if specific to only one of these motor phenotypes and if they incorporate differentiating aspects of dystonia and spasticity clinical consensus definitions.

The Hoffman (H) reflex is related to the tendon stretch reflex and can measure hyperreflexia. H-reflex amplitude and suppression with high frequency stimulation track with spasticity severity in rats with spinal cord injury and in spastic children and adults with spinal cord injury, stroke, and CP (Chen et al., 2001; Garrison et al., 2011; Hoving et al., 2006; Kumru et al., 2015; Pizzi et al., 2005; Ryu et al., 2017; Tekgül et al., 2013; Yates et al., 2008). Similar H-reflex abnormalities are not observed in dystonic adults (Koelman et al., 1995), thus offering specificity for spasticity.

Electromyographic determinations of overflow muscle activation during voluntary movement can identify dystonia. Theta band coherence between antagonist muscles is seen inconsistently in dystonic adults (Chaniary et al., 2008; Choudhury et al., 2018; De Bruijn et al., 2017; Foncke et al., 2007; Grosse et al., 2004; Nijmeijer et al., 2014; Tijssen et al., 2002) and not at all in spastic adults (Chen et al., 2018). Therefore, its presence is supportive of dystonia but its absence does not imply absence of dystonia. Cross-correlation between

antagonist muscles is elevated in adults with focal dystonia (Farmer et al., 1998) and in a genetic rat model of dystonia (DeAndrade et al., 2016) but has not been extensively studied in spasticity. To increase the specificity of these measures for dystonia, their association with the H-reflex and different arousal states can be examined. Since dystonia is not typically associated with hyperreflexia, a measure specific for dystonia should not correlate with H-reflex measures. Furthermore, a measure specific for dystonia should be greater when awake compared to when sedate, which is not as characteristic of spasticity.

Here, we describe a model of global neonatal hypoxic injury in rats that demonstrates subtle motor impairment and electrophysiologic features of dystonia and spasticity, as would be seen in CP. Interestingly, this model suggests that female sex may be a risk factor for developing dystonia while male sex may be a risk factor for developing spasticity following neonatal brain injury in rats.

2. Materials and methods

2.1. Animals

All procedures were approved by the Beth Israel Deaconess Medical Center Institutional Animal Care and Use Committee. Timed pregnant Sprague Dawley dams were obtained from Charles River at embryonic days 17–18. Pups were born between embryonic days 21–23. Pups were aged within a 12-hour window from the time of birth and weaned at post-natal day (P) 21.

2.2. Neonatal brain injury

Pups were randomized to global hypoxia or sham exposure between P7 and P8 at a 2:1 hypoxia:sham ratio (anticipating some mortality with hypoxia exposure). An airtight hypoxia chamber (BioSpherix Ltd., Parish, NY) was used to expose pups to graded global hypoxia over 12 min beginning at room air (21% oxygen) and culminating in anoxia. Sham exposure involved placement of the pup in the chamber for 12 min at room air. Pups precipitously drop their heart rate (as determined by surface electrocardiography) between 4 and 6 min into the hypoxia exposure and also decrease their temperature (determined via rectal temparature probe) as is typical of neonatal hypoxic ischemic injury in humans (Burnard and Cross, 1958) (Fig. 1A). Pups exhibit generalized clonic and myoclonic activity at 3 min, exhibit hypermotor activity at 4 min, and then cease movement at 6 min into the exposure. Pups are then placed individually on a flat surface in room air for 8 min before being returned to the dam. By this time, pups are pink and have resumed spontaneous movement or are deceased.

P7-8 was chosen as the age range for hypoxia exposure after trialing exposure across P5-P10, corresponding to human 35–40 postconceptional weeks based on brain growth rate (Clancy et al., 2007; Dobbing and Sands, 1979), noting that neonatal brain injury at term gestation may be most clinically likely to yield dystonia in addition to spasticity (Himmelmann et al., 2009). Pups exposed at P9–10 ($n = 3$) died immediately following the exposure. Pups undergoing exposure at P5–6 ($n = 4$) did not develop gait or rotarod performance impairment.

Data collection and analysis was performed with the investigators blinded to the sex and hypoxia exposure status of the pups.

2.3. Motor functional characterization

Motor activity was examined between P27-29, equivalent to human late childhood/adolescence (Clancy et al., 2007; Dobbing and Sands, 1979). This time point was chosen given the clinical delay in dystonia emergence following neonatal brain injury and to ensure that dystonia emerges prior to adulthood as typical for CP (Himmelmann et al., 2009; Lin et al., 2014).

Rotarod performance was assessed on an accelerating rotarod (AccuRotor Rotarod, Omnitech Electronics, Columbus, OH, 70 mm rod diameter, 40 cm fall height). Rats were acclimated to the stationary rotarod for ten 3-minute trials and then to the rotating rod at 4 rotations-per-minute for five 3-minute trials. For testing, rotarod acceleration linearly increased from 4 to 40 rotations-per-minute over 3 min for each of three trials. The maximum latency to fall across all three trials was used for further analysis. Rats had 10-minute rest periods between the three acclimation/testing sessions and 1-minute rest periods between trials.

Gait performance was evaluated during native gait across a clear plexiglass walkway (36 in. long by 3 in. wide by 10 inches tall with an open top). Rats were acclimated to this walkway for 15 min prior to testing. For gait analysis trials, room lights were dimmed, a bright lamp was placed at one end of the walkway, and the other end of the walkway was opened to a red tinted box covered with an opaque drape. Rats were placed at the brightly lit end of the walkway and spontaneously traversed the box to the darkened end for three trials. Epochs of 5 continuous gait cycles without pauses for grooming or exploration were analyzed. Gait data was excluded if the animal paused too frequently across the three trials to observe a continuous 5 gait cycle epoch. Three representative gait cycles across the three trials during periods of continuous gait were analyzed for stride length, stride duration, and speed. Videos recorded from underneath the walkway were manually scored by two investigators blinded to the hypoxia exposure status of the pups (SG and BA) with 25% of all videos examined by both investigators to ensure comparable scoring.

2.4. Electrophysiologic recordings

Electrophysiologic measures of dystonia and spasticity were performed between P28-30 (TECA Synergy T2 System, Viasys, Madison, WI), on the day following motor behavioral characterization.

H-reflexes were elicited in isoflurane-sedated rats such that vibrissae and whisking reflexes were absent (isoflurane 0.5 to 1% *v*/v in oxygen). Two monopolar stimulating electrodes (Natus TECA electrodes, 1 inch length, 0.36 mm diameter) were inserted on the medial and lateral edges of the calcaneal tendon to stimulate the tibial nerve. The H-reflex was recorded 5–8 msec after the stimulus (pulse width 0.2 msec, amplitude 0.5–3 mA) in the plantar interossei between the fourth and fifth metatarsals (Yates et al., 2008). H-reflexes were elicited at 0.2 Hz, then at 2 Hz, then again at 0.2 stimulation frequencies to examine

H-reflex suppression. At least five responses were elicited at each stimulus frequency to ensure stable H-reflex amplitude before recording five H-reflex responses for analysis.

Coherence was determined from continuous bipolar electromyography (EMG) signals simultaneously recorded in the tibialis anterior and triceps surae complex (containing both the gastrocnemius and soleus muscles). These muscles were chosen as foot inversion and plantar flexion are commonly observed in dystonia and are subserved by these antagonist muscles (Sanger and Ferman, 2017; Schneider et al., 2006). EMG was recorded with a 30 kHz sampling frequency with filter settings of 0.1 to 10 kHz with a 60 Hz notch filter. Signals were stored digitized at 1000 Hz sampling frequency. Two needle electrodes (Ambu Neuroline Subdermal Twisted Pair, Columbia, MD) were placed 1 mm apart in each muscle belly at approximately 1/3 the distance between the patella and calcaneus. Isoflurane was maintained at 2% *v*/v in oxygen during needle insertion, ensuring that vibrissae, whisking, and pedal reflexes were absent. Needle electrodes were secured and the rat and hindlimb were restrained with micropore tape. Anesthesia was then turned off. Pressure was applied using a bulldog clip to the base of the tail once every 2 s. Thirty seconds following anesthesia discontinuation, rats would respond to tail pressure with hindlimb withdrawal attempts, resulting in the isometric contraction of multiple hindlimb muscles. Tail pressure was applied at the same frequency for an additional 100 s after the first voluntary movement. The rats were then re-anesthetized for removal of the electrodes and restraints.

2.5. Signal processing

H-reflex amplitude was calculated as the voltage difference between the most negative and most positive portions of the H-reflex waveform, relative to a level baseline. The ratio of the average H-reflex amplitude at 2 Hz to the average amplitude at 0.2 Hz quantified the degree of H-reflex suppression. Ratios approximating 1 indicate no suppression while ratios approximating 0 indicate complete suppression of the H-reflex with 2 Hz stimulation (Fig. 1B). The higher the ratio, the greater the hyperreflexia (Garrison et al., 2011; Yates et al., 2008).

H-reflex data was excluded if the repeat H-reflex amplitude measure at 0.2 Hz was > 10% different from the original H-reflex amplitude measurement at 0.2 Hz or if the H-reflex could not be elicited within 15 min of achieving the appropriate anesthetic plane.

Theta band coherence and cross-correlation values at zero lag were determined for each animal during the first and last 15 s of EMG recording (sedate and awake periods, respectively) over the 100 s recording period. These measures were calculated offline (MATLAB, MathWorks, Natick, MA) using methods that have been previously described in adult patients with dystonia(Grosse et al., 2004). Digitized EMG signals were high-pass filtered at 65 Hz and then rectified. This preserves motor unit data (which occurs at frequencies > 100 Hz) but removes electrical noise and low frequency baseline deviations representative of movement and wire capacitance artifact(Grosse et al., 2004). To convert EMG signals from multi-unit motor unit activity to point processes, EMG was leveled relative to the amplitude of the background signal. EMG signal exceeding 5 standard deviations above the mean of 250 milliseconds of representative signal baseline was set at a value of 1 with the remainder of the signal set at 0. This leveling process preserves the

temporal information of motor unit firing while eliminating effects of volume conduction from surrounding muscles. Notably, temporal information about motor unit firing is the key comparator between antagonist muscles to determine whether there is overflow activation.

EMG recordings were excluded if motor unit activity could not be reliably differentiated from background activity.

Coherence was calculated using *mscoher* in MATLAB (window length 1024, no overlap, 0.98 Hz frequency resolution). Coherence describes the spectral distribution of the oscillatory synchrony between two signals and ranges from 0 to 1 with 0 indicating no synchrony and 1 indicating complete synchrony at a given frequency. The Fisher z-transformation was applied to yield constant variance across records. Of note, this transformed coherence can yield values > 1. Transformed coherence between the tibialis anterior and triceps surae complex EMG was summed between 4 and 7 Hz (theta band) and compared across animals (Fig. 1C).

Cross-correlation was calculated using *xcorr* in MATLAB. Given that restrained isometric hindlimb withdrawal was examined, there was co-contraction between antagonist muscles in all animals with peak cross-correlogram values occurring near zero lag between EMG signals. The cross-correlation amplitude at zero lag was compared across animals, with higher values indicating greater temporal synchrony between antagonist muscles (Fig. 1C). The cross-correlation amplitude was divided by the total duration of movement in the analyzed epoch to allow comparison between animals who displayed differences in muscle contraction duration or frequency of hindlimb withdrawals (DeAndrade et al., 2016). The Fisher z-transform was then applied to yield a constant variance across records (DeAndrade et al., 2016).

The application of the rectification and leveling process to EMG signals eliminates all contribution of EMG amplitude discrepancies between animals which could be affected by subtle differences in electrode placement and muscle size (Grosse et al., 2004). This allows us to compare the amplitude of the derived cross-correlograms across animals, noting that this distribution has been normalized with the Fisher z-transform (DeAndrade et al., 2016).

2.6. Statistical analysis

Repeated measure ANOVA was used to assess variability of hypoxia exposure across pups (repeated measures general linear model, SPSS, IBM, Armonk, NY). Functional and electrophysiologic motor data was first analyzed using MANOVA (multivariate general linear model, SPSS) to assess the effect of two independent variables on multiple dependent motor outcome variables. Hypoxia exposure (vs. sham exposure) and sex were set as independent variables. Rotarod latency to fall, stride length, stride duration, speed, H-reflex suppression ratio, theta band coherence when awake, theta band coherence when sedate, cross-corelation when awake, and cross-correlation when sedate were set as dependent variables. MANOVA Pillai's trace $p < .05$ was deemed significant for main effects and interactions. Levene's F-tests was used to confirm homogeneity of variance across groups ($p > .05$) before employing post-hoc comparisons via Tukey's HSD with significance cutoff of $p < .05$. Two-tailed, one-sample *t*-tests were employed to compare motor measure

values against expected reference values. Pearson correlations were used to compare the relationship between electrophysiologic measures of spasticity and dystonia. Population summary values are indicated as 95% confidence intervals (CI) based on the normal distribution.

3. Results

3.1. Animal numbers and reproducibility of hypoxia exposure

In total, 75 pups across 6 litters were randomized to hypoxia (51 pups) vs. sham exposure (24 pups). Eight pups succumbed to the hypoxia exposure. The remaining 43 pups were returned to the dam and thrived without further special intervention. Hypoxia-exposed pups could not be visually differentiated from sham-exposed litter mates within 24 h of the initial exposure. There was no difference in weight ($p = .1$) at the time of motor characterization (P27-P29) between hypoxia (95% CI 85.8–93.2 g) and sham-exposed rats (95% CI 87.0–106 g).

Hypoxia exposure was reproducible across pups as there was almost no variability between pups in vital signs during hypoxia exposure. Specifically, there was no difference between males and females in temperature, heart rate (as evaluated by QRS complexes/min), or ambient fraction of inspired oxygen at 3, 6, 9, or 12 min following hypoxia onset (repeated measures ANOVA, $p = 1$).

Data exclusion rates were comparable irrespective of sex and hypoxia exposure status except regarding gait analysis, where more sham-exposed rats were excluded compared to hypoxia-exposed rats for frequent grooming and exploration behavior (chi square with Yates correction $p = .04$) (Table 1).

3.2. Hypoxia exposure yields sex-dependent functional and electrophysiologic motor abnormalities

A statistically significant MANOVA effect was obtained when comparing sham and hypoxia-exposed rats across all assessed motor functional and electrophysiologic measures (Pillai's trace F = 5.28, $p < .0005$). There was a statistically significant effect of sex (Pillai's trace F = 2.72, $p = .01$) with a significant interaction between hypoxia exposure and sex (Pillai's trace F = 2.546, $p = .02$), suggesting that motor measures were affected by hypoxia in a sex-dependent manner. Subsequent post-hoc tests compared responses between hypoxia and sham-exposed pups of each sex. Table 1 indicates these results comprehensively, separated by hypoxia exposure and sex.

3.3. Hypoxia exposure yields subtle motor impairment, perhaps more so in males

Hypoxia-exposed animals had significantly shorter stride lengths than did sham-exposed animals ($p = .02$), without a significant difference in stride duration, speed, or rotarod performance. When examining each sex separately, only males manifested motor impairment after hypoxia exposure but only with diminished rotarod performance ($p = .02$). Females did not display significant differences between hypoxia and sham exposure in the tested motor functional measures (Table 1, Fig. 2). Notably, none of these functional

motor measures correlated with H-reflex or cross-correlogram measures ($p > .2$, Pearson correlation).

3.4. Hypoxia exposure yields electrophysiological markers of spasticity, predominantly in males

The H-reflex demonstrated suppression at 2 Hz in sham-exposed animals with ratios significantly < 1 (95% CI 0.303–0.637, two-tailed one-sample *t*-test, $p < .0001$). Hypoxia-exposed animals also displayed H-reflex suppression at 2 Hz (95% CI 0.719–0.992, two-tailed one-sample *t*-test, p = .04) but had reduced suppression compared to sham-exposed animals ($p = .002$), as would be seen with spasticity. When examining H-reflex suppression within each sex, only males demonstrated diminished H-reflex suppression following hypoxia (p = .02), while females did not ($p = 1.0$, Table 1, Fig. 3A). Of note, in sham-exposed animals, there is a trend showing that females have diminished H-reflex suppression compared to males. Though this trend did not reach significance ($p = .8$, MANOVA with post-hoc Tukey HSD), it is suggestive of a phenomenon also observed in human subjects (Hoffman et al., 2018).

3.5. Hypoxia exposure yields electrophysiological markers of dystonia, predominantly in females

There was no difference between sham and hypoxia-exposed animals in 4–7 Hz coherence regardless of arousal state. In contrast, cross-correlogram values were significantly higher in hypoxia-exposed animals compared to sham-exposed animals when awake (p = .002), but not when sedated ($p = .1$). Females exhibited the same significant difference when awake (p = .02), but this difference did not reach significance in males ($p = .08$). This contrasts with the sex differences seen with motor function and spasticity measures, where males displayed differences between hypoxia and sham exposure while females did not (Table 1, Fig. 3B).

3.6. Electrophysiologic markers of spasticity and dystonia are independent

Cross-correlation can be a marker of overflow muscle activation during voluntary movement as would be seen in dystonia or can be a marker of co-contraction between antagonist muscles regardless of voluntary movement trigger as can be seen in spasticity. Given that the H-reflex is associated with spasticity and has been used as a marker of spasticity severity, correlation between H-reflex and cross-correlation values would suggest that cross-correlation could also be a feature of spasticity. However, there is no significant correlation between H-reflex suppression and cross-correlation amplitude (Pearson correlation R^2 = 4.86e-6, p = 1 for sham-exposed animals; R^2 = 2.22e-3, $p = .4$ for hypoxia-exposed animals) (Fig. 4A).

3.7. Hypoxia exposure mostly yields mixed spasticity and dystonia

H-reflex measures and cross-correlation measures for both sham-exposed and hypoxia-exposed animals lay on a continuum. Using an exploratory and descriptive approach to characterize the range of electrophysiologically-defined motor phenotypes in these animals, we determined the upper limits of the 95% confidence intervals (CI) of H-reflex suppression (a ratio of 0.637) and cross-correlation values (0.798 μV) in sham-exposed animals. We

used these values as cut-offs for suggesting which of the hypoxia-exposed animals could be thought of as having more electrophysiologically spastic or dystonic features (Table 1). Based on these criteria, 27/41 animals in whom H-reflex suppression data was available could be thought to have spastic features and 28/42 animals in whom cross-correlation data was available could be thought to have dystonic features. Of these, 18 animals displayed both spastic and dystonic features such that that 9/41 animals were predominantly spastic, and 10/42 animals were predominantly dystonic. Only 5 hypoxia-exposed animals had H-reflex and cross-correlation measures within the 95% CI of sham values and may be thought of as least affected by neonatal brain injury (Fig. 4B). Of note, as these values all lie on a continuum, some sham-exposed animals also qualified as having dystonic or spastic features by the above utilized criteria. Therefore, this method cannot be used as a definitive way to classify motor phenotype but can be used to characterize the spread of abnormalities that can be seen in this model following neonatal hypoxia.

4. Discussion

We have described a clinically-relevant rat model of neonatal brain injury that demonstrates electrophysiologic markers of dystonia and spasticity. Most animals display a mixed spastic and dystonic phenotype, though some animals display predominantly dystonia or spasticity. The model also suggests a possible sexual dichotomy in motor outcomes, with males displaying significantly elevated spasticity measures while females did not. Females displayed significantly elevated dystonia measures while this difference did not reach significance in males.

4.1. Limitations

Sex was not originally considered as a part of the randomization process. This led to a disproportionately high number of female relative to male sham-exposed pups. There does appear to be a trend suggesting that males also have higher cross-correlogram peak amplitudes after hypoxia, though this did not reach significance. For these reasons, it is difficult to say that males do not display electrophysiologic markers of dystonia following neonatal hypoxia in this animal model. However, females do clearly display electrophysiologic markers of dystonia and not spasticity after neonatal hypoxia.

There are trends toward male sham-exposed mice having lower baseline values on spasticity and dystonia measures compared to female sham-exposed mice. However, none of these trends reach significance and there is considerable overlap in these values when comparing the sexes. It is possible that males do in fact have lower baseline values on the examined measures compared to females (Hoffman et al., 2018) and that this may become apparent with a larger number of animals. However, any possible sex differences in these values at baseline would only further highlight the importance in considering sex as a critical variable in motor outcomes following neonatal brain injury. This supports segregation by sex when comparing these motor outcomes and further validates comparing hypoxia-exposed animals to sham-exposed animals of the same sex, as we have done.

This model presents an alternative to the more commonly used Rice-Venucci model of neonatal brain injury which involves the application of global hypoxia following unilateral

or bilateral carotid artery ligation. The Rice-Vanucci model is known to produce significant neuronal injury (Rumajogee et al., 2016). There is an existing body of evidence that global hypoxia alone may not yield significant neuronal injury in rodents, though it can produce significant functional pathology like seizures (Sun et al., 2016). The study of animal models of cerebral palsy have often focused on the mechanisms underlying neuronal injury following hypoxia and ischemia. However, we feel that our model instead appropriately focuses on replication of the most common cerebral palsy motor phenotypes first before examining the relevant pathophysiology underlying these phenotypes. Furthermore, using global hypoxia as the etiology of neonatal brain injury in this model may be more broadly clinically relevant than the stroke-like insults induced with carotid artery ligation (SCPE, 2002). Therefore, though histology may or may not yield clear cut differentiation between phenotypes in this model, the spasticity and dystonia phenotypes remain objectively identifiable and clinically relevant, making this model ripe for a wide range of investigations of spasticity and dystonia pathophysiology following neonatal brain injury.

We do not characterize the non-motor sequelae of neonatal brain injury in this model. Though seizure-like activity was consistently seen during the hypoxia exposure (repeated clonic and isolated myoclonic jerks), this was not observed subsequently. Though hypoxia this severe has been attempted previously and not been shown to yield a viable seizure phenotype(Sun et al., 2016), future characterization of this model could employ chronic electroencephalography to assess for subtle seizures. Intellectual disability is another common comorbidity in CP(Himmelmann et al., 2009). It is possible that exploratory behaviors were reduced in this model post-hypoxia (see Methods). Therefore, cognitive behavioral assessments could also be a worthwhile.

4.2. Validity of electrophysiologic measures of spasticity and dystonia

Our results show that neonatal hypoxia yields increased cross-correlation between antagonist muscle EMG during voluntary movement and that this is potentiated by arousal, replicating key clinical features of dystonia. Though it is possible that antagonist muscle cross-correlation could also be suggestive of spasticity, potentiation with arousal and absence of significant correlation between cross-correlogram peak amplitude and H-reflex suppression suggests that cross-correlation between antagonist muscles as measured here is an independent marker of dystonia. These measures were chosen in large part for their clinical relevance. Both have been used in patients to effectively assess dystonia (Farmer et al., 1998) and spasticity (Hoving et al., 2006; Kumru et al., 2015; Pizzi et al., 2005; Tekgül et al., 2013).

Theta band coherence was not seen following neonatal hypoxic injury. Given that theta band coherence is inconsistently observed following dystonia (Chaniary et al., 2008; Choudhury et al., 2018; De Bruijn et al., 2017; Foncke et al., 2007; Grosse et al., 2004; Nijmeijer et al., 2014; Tijssen et al., 2002) and is absent in adult patients with dystonia following neonatal brain injury (Grosse et al., 2004), its absence in this model does not imply an absence of dystonia.

Alpha band oscillatory activity within muscles is another electrophysiologic measure previously examined in dystonia and spasticity during voluntary movement tasks. However,

intramuscular alpha band oscillatory activity decreases in both dystonia and spasticity making it non-specific for either phenotype (Bravo-Esteban et al., 2014; Nijmeijer et al., 2014). It was, therefore, not assessed here.

Interestingly, cross-correlation amplitude trended toward a mild decrease in sham-exposed animals as they recovered from anesthesia. Transient hypertonia with emergence from inhalational anesthetics is a well-described clinical phenomenon (Azar et al., 1984; McCulloch and Milne, 1990; Rosenberg et al., 1981). The fact that this phenomenon is loosely reflected in our data and, furthermore, the fact that it contrasts with the increase in cross-correlation amplitude seen with hypoxia-exposed animals, highlights the clinical validity of this cross-correlation measure.

H-reflex suppression is a measure of hyperreflexia and not a direct measure of spasticity. However, H-reflex measures have been shown to track with spasticity severity (Hoving et al., 2006; Kumru et al., 2015; Pizzi et al., 2005; Tekgül et al., 2013). Furthermore, hyperreflexia is a component of upper motor neuron injury (Sanger et al., 2010) and is often used as an adjunct to differentiate between spasticity and dystonia clinically, particularly in infants where passive range of motion assessments at different velocities of stretch can be difficult to accomplish reliably. Future characterization of the model could quantify resistance to passive joint stretch at different velocities in anesthetized animals as an additional measure of spasticity.

A critical limitation is our inability to clearly correlate these electrophysiologic measures with evidence of motor disability. Functional motor testing in this model revealed only very subtle motor impairment (diminished stride length). When examining the sexes separately, a subtle motor impairment was present only in males but in a different functional motor measure (shorter latency to fall of an accelerating rotarod). Given that cross-correlogram and H-reflex measures have been previously correlated to motor impairment in both patients and animal models (Chen et al., 2001; Farmer et al., 1998; Garrison et al., 2011; Hoving et al., 2006; Kumru et al., 2015; Pizzi et al., 2005; Ryu et al., 2017; Tekgül et al., 2013; Yates et al., 2008), it is likely that our inability to correlate these measures to motor impairment in this model is predominantly a reflection of the relatively minor motor impairment.

4.3. Clinical relevance of the model

Neonatal brain injury that leads to dystonia typically occurs at term-equivalent gestation and is associated with a sudden and severe insult that involves hypoxia and ischemia (e.g. placental abruption) (Himmelmann et al., 2009). To mimic this, graded global hypoxia culminating in anoxia was applied to pups at post-natal day 7–8, equivalent to human term gestation (Clancy et al., 2007; Dobbing and Sands, 1979). Global ischemia likely occurred for the last 7 of the 12 min of hypoxia exposure, coincident with the precipitous drop in heart rate from > 350 QRS complexes/min to < 30 QRS complexes/min. The largest limitation in the clinical relevance of this model is that rat pups are *ex utero* for hypoxia exposure while, clinically, neonatal brain injury leading to dystonia typically happens in utero or during delivery. This is an insurmountable and critical difference in establishing a rodent model of neonatal brain injury at term equivalent gestation. Pups were also allowed to self-regulate their temperature during the hypoxia exposure and cooled. Though this is

a physiologically observed phenomenon (Burnard and Cross, 1958), it may be worthwhile to modify the hypoxia exposure such that pups are maintained at 37 °C to better mimic the temperature of the in utero environment. Increased core temperature has been associated with greater injury burden (Wood et al., 2017) and may result in greater mortality but also a more severe phenotype.

4.4. Sex differences and implications for pathophysiology

Males display diminished H-reflex suppression following neonatal hypoxia suggestive of spasticity. Females display increased antagonist muscle cross-correlation following neonatal hypoxia suggestive of dystonia. Therefore, it may be worth exploring whether sex could at least partially affect electrophysiologic motor phenotype after neonatal brain injury.

It is unclear whether a similar difference is present clinically. Population-based epidemiologic data can be tainted by inconsistent characterization of CP subtype between practitioners, the known under-recognition of dystonia in CP, and great variability in neonatal brain injury mechanism and postnatal care between children (Aravamuthan and Waugh, 2016; Eggink et al., 2017; Lin et al., 2014; Rice et al., 2017). Noting these limitations, there have not yet been detailed epidemiological studies comparing risk factors for spastic and dystonic CP, though a small study suggests that there is a female predominance amongst children with dystonic CP (Westbom et al., 2007). To determine the clinical relevance of the sex differences we have described, it will be critical to examine the long-term motor sequelae of children with comparable mechanisms of injury at term gestation.

There is extensive animal and clinical literature suggesting that males are more affected than females by neonatal brain injury (Clowry et al., 2014; SCPE, 2002; Sharma et al., 2014). However, our results suggest the electrophysiological motor abnormalities seen in females (namely dystonia) may be overlooked with conventional testing measures in other studies. This is particularly notable when considering that many rodent models of dystonia have no observable motor phenotype (Oleas et al., 2013; Shakkottai et al., 2017). It is possible that these models may instead display and electrophysiologic dystonia phenotype (DeAndrade et al., 2016). Our results showing electrophysiologic differentiation between dystonia and spasticity suggest a way forward in looking for more subtle but still objectively quantifiable motor abnormalities in neonatal brain injury and genetic dystonia animal models. H-reflex and cross-correlation could serve as biomarkers for symptom severity and therapeutic effect in models of spasticity and dystonia which don’t otherwise display motor disability.

In rodent models of neonatal brain injury, males have historically displayed a higher injury burden (Clowry et al., 2014; Johnston and Hagberg, 2007). These animal model observations are borne out epidemiologically, as there are more males with CP than there are females (SCPE, 2002).

Though much of the literature in animal models of neonatal brain injury describes greater neuronal dysfunction in males following hypoxia, mitochondrial biogenesis following hypoxia is more impaired in females (Demarest and McCarthy, 2015; Sharma et al., 2014). This is particularly noted in the cerebellum, a possible node of dysfunction in

dystonia (Demarest and McCarthy, 2015; Shakkottai et al., 2017; Sharma et al., 2014). Future research could also investigate the role of sex-dependent differences in post-hypoxia mitochondrial biogenesis in dystonia following neonatal brain injury.

4.5. Future directions

Dystonia was assessed only by examining co-contraction between the triceps surae complex and tibialis anterior, largely because foot inversion and plantar flexion is a commonly seen dystonia phenotype (Sanger and Ferman, 2017; Schneider et al., 2006). It is possible that dystonia is present, or may even be more apparent, in other muscle groups. This could be investigated by engaging these muscles in other, more complex, motor tasks like voluntary gait.

Animals were assessed during a narrow age range to ensure comparability between animals and to ensure capture of the most likely timepoint of dystonia emergence based on extrapolation from clinical observations. However, longitudinal assessment of motor impairment in this model would be valuable to establish a timeline for when motor abnormalities develop and to determine whether abnormalities remain stable over time. The latter would be particularly valuable if this model were to be used to test potential therapeutics for CP.

It would be interesting to compare the electrophysiolgic motor phenotypes characterized in the model presented here with electophysiologic motor phenotypes in the more typically used carotid ligation plus global hypoxia stroke-like models of neonatal brain injury. It is possible that neonatal brain injury models employing carotid artery ligation also display spasticity and dystonia phenotypes that cannot clearly be discerned without objective electrophysiologic characterization.

Detailed histological characterization of this model as discussed above should involve differentiation between neuronal subtypes and basal ganglia structures (Aravamuthan and Waugh, 2016). As striatal cholinergic interneurons have been commonly functionally implicated in dystonia pathogenesis, these neurons should be specifically studied (Eskow Jaunarajs et al., 2015). Electrophysiological characterization of changes to basal ganglia firing and local field potential activity in this model can help inform deep brain stimulation target selection and stimulation parameters. Dissection of neural circuit abnormalities differentiating between dystonia and spasticity using optogenetic and chemogenetic techniques could also be pursued, particularly given the emergence of genetic Cre-recombinase rat lines. Therefore, this model, perhaps for the first time, provides a controlled substrate for examining the differences in the pathophysiology and treatment of spasticity and dystonia following neonatal brain injury.

Acknowledgments

Funding

Funding supporting this work is from the National Institutes of Neurological Disorders and Stroke (3R25NS070682-07S1, 5K12NS098482-02). There are no conflicts of interest.

Abbreviations:

CP	cerebral palsy
H-reflex	Hoffman reflex
EMG	electromyography
P	postnatal day

References

Albanese A, Bhatia K, Bressman SB, Delong MR, Fahn S, Fung VSC, Hallett M, Jankovic J, Jinnah HA, Klein C, Lang AE, Mink JW, Teller JK, 2013. Phenomenology and classification of dystonia: a consensus update. Mov. Disord 28, 863–873. 10.1002/mds.25475. [PubMed: 23649720]

Aravamuthan BR, Waugh JL, 2016. Localization of basal ganglia and thalamic damage in dyskinetic cerebral palsy. Pediatr. Neurol 54, 11–21. 10.1016/j.pediatrneurol.2015.10.005. [PubMed: 26706479]

Ashwal S, Russman BS, Blasco PA, Miller G, Sandler A, Shevell M, Stevenson R, 2004. Practice parameter: diagnostic assessment of the child with cerebral palsy: report of the Quality Standards subcommittee of the American Academy of Neurology and the Practice Committee of the Child Neurology Society. Neurology 62, 851–863. [PubMed: 15037681]

Azar I, Karambelkar DJ, Lear E, 1984. Neurologic state and psychomotor function following anesthesia for ambulatory surgery. Anesthesiology 60, 347–349. [PubMed: 6703389]

Bravo-Esteban E, Taylor J, Aleixandre M, Simon-Martínez C, Torricelli D, Pons JL, Gómez-Soriano J, 2014. Tibialis anterior muscle coherence during controlled voluntary activation in patients with spinal cord injury: diagnostic potential for muscle strength, gait and spasticity. J. Neuroeng. Rehabil 11, 23. 10.1186/1743-0003-11-23. [PubMed: 24594207]

Burnard ED, Cross KW, 1958. Rectal temperature in the newborn after birth asphyxia. Br. Med. J 2, 1197–1199. [PubMed: 13584896]

Chaniary K, Baron M, Rice A, Wetzel P, Shapiro S, 2008. Electromyographic characterization in an animal model of dystonia. Mov. Disord 23, 1122–1129. 10.1002/mds.22040. [PubMed: 18442136]

Chen XY, Feng-Chen KC, Chen L, Stark DM, Wolpaw JR, 2001. Short-term and medium-term effects of spinal cord tract transections on soleus H-reflex in freely moving rats. J. Neurotrauma 18, 313–327. 10.1089/08977150151070973. [PubMed: 11284551]

Chen Y-T, Li S, Magat E, Zhou P, Li S, 2018. Motor overflow and spasticity in chronic stroke share a common pathophysiological process: analysis of within-limb and between-limb EMG-EMG coherence. Front. Neurol 9, 795. 10.3389/fneur.2018.00795. [PubMed: 30356703]

Choudhury S, Singh R, Chatterjee P, Trivedi S, Shubham S, Baker MR, Kumar H, Baker SN, 2018. Abnormal blink reflex and intermuscular coherence in Writer's cramp. Front. Neurol 9, 517. 10.3389/fneur.2018.00517. [PubMed: 30013510]

Clancy B, Finlay BL, Darlington RB, Anand KJS, 2007. Extrapolating brain development from experimental species to humans. Neurotoxicology 28, 931–937. 10.1016/j.neuro.2007.01.014. [PubMed: 17368774]

Clowry GJ, Basuodan R, Chan F, 2014. What are the best animal models for testing early intervention in cerebral palsy? Front. Neurol 5, 258. 10.3389/fneur.2014.00258. [PubMed: 25538677]

De Bruijn E, Nijmeijer SWR, Forbes PA, Koelman JHTM, Van Der Helm FCT, Tijssen MAJ, Happee R, 2017. Dystonic neck muscles show a shift in relative autospectral power during isometric contractions. Clin. Neurophysiol 128, 1937–1945. 10.1016/j.clinph.2017.06.258. [PubMed: 28826024]

DeAndrade MP, Trongnetrpunya A, Yokoi F, Cheetham CC, Peng N, Wyss JM, Ding M, Li Y, 2016. Electromyographic evidence in support of a knock-in mouse model of DYT1 dystonia. Mov. Disord 31, 1633–1639. 10.1002/mds.26677. [PubMed: 27241685]

Demarest TG, McCarthy MM, 2015. Sex differences in mitochondrial (dys)function: implications for neuroprotection. J. Bioenerg. Biomembr 47, 173–188. 10.1007/s10863-014-9583-7. [PubMed: 25293493]

Dobbing J, Sands J, 1979. Comparative aspects of the brain growth spurt. Early Hum. Dev 3, 79–83. [PubMed: 118862]

Dressier D, 2011. Nonprimary dystonias. Handb. Clin. Neurol 100, 513–538. 10.1016/B978-0-444-52014-2.00038-0. [PubMed: 21496605]

Eggink H, Kremer D, Brouwer OF, Contarino MF, van Egmond ME, Elema A, Folmer K, van Hoorn JF, van de Pol LA, Roelfsema V, Tijssen MAJ, 2017. Spasticity, dyskinesia and ataxia in cerebral palsy: are we sure we can differentiate them? Eur. J. Paediatr. Neurol 10.1016/j.ejpn.2017.04.1333.

Eskow Jaunarajs KL, Bonsi P, Chesselet MF, Standaert DG, Pisani A, 2015. Striatal cholinergic dysfunction as a unifying theme in the pathophysiology of dystonia. Prog. Neurobiol 127–128, 91–107. 10.1016/j.pneurobio.2015.02.002.

Farmer SF, Sheean GL, Mayston MJ, Rothwell JC, Marsden CD, Conway BA, Halliday DM, Rosenberg JR, Stephens JA, 1998. Abnormal motor unit synchronization of antagonist muscles underlies pathological co-contraction in upper limb dystonia. Brain 121 (Pt 5), 801–814. [PubMed: 9619186]

Fehlings D, Brown L, Harvey A, Himmelmann K, Lin J-P, Macintosh A, Mink JW, Monbaliu E, Rice J, Silver J, Switzer L, Walters I, 2018. Pharmacological and neurosurgical interventions for managing dystonia in cerebral palsy: a systematic review. Dev. Med. Child Neurol 60, 356–366. 10.1111/dmcn.13652. [PubMed: 29405267]

Foncke EMJ, Bour LJ, van der Meer JN, Koelman JHTM, Tijssen MAJ, 2007. Abnormal low frequency drive in myoclonus-dystonia patients correlates with presence of dystonia. Mov. Disord 22, 1299–1307. 10.1002/mds.21519. [PubMed: 17486590]

Garrison MK, Yates CC, Reese NB, Skinner RD, Garcia-Rill E, 2011. Wind-up of stretch reflexes as a measure of spasticity in chronic spinalized rats: the effects of passive exercise and modafinil. Exp. Neurol 227, 104–109. 10.1016/j.expneurol.2010.09.019. [PubMed: 20932828]

Grosse P, Edwards M, Tijssen MAJ, Schrag A, Lees AJ, Bhatia KP, Brown P, 2004. Patterns of EMG-EMG coherence in limb dystonia. Mov. Disord 19, 758–769. 10.1002/mds.20075. [PubMed: 15254933]

Himmelmann K, McManus V, Hagberg G, Uvebrant P, Krageloh-Mann I, Cans C, 2009. Dyskinetic cerebral palsy in Europe: trends in prevalence and severity. Arch. Dis. Child 94, 921–926. 10.1136/adc.2008.144014. [PubMed: 19465585]

Hoffman M, Norcross M, Johnson S, 2018. The Hoffmann reflex is different in men and women. Neuroreport 29, 314–316. 10.1097/WNR.0000000000000961. [PubMed: 29293170]

Hoving MA, van Kranen-Mastenbroek VHJM, van Raak EPM, Spincemaille GHJJ, Hardy ELM, Vies JSH, 2006. Placebo controlled utility and feasibility study of the H-reflex and flexor reflex in spastic children treated with intrathecal baclofen. Clin. Neurophysiol 117, 1508–1517. 10.1016/j.clinph.2006.04.014. [PubMed: 16759902]

Johnston MV, Hagberg H, 2007. Sex and the pathogenesis of cerebral palsy. Dev. Med. Child Neurol 49, 74–78. 10.1111/j.1469-8749.2007.0199a.x. [PubMed: 17209983]

Koelman JH, Willemse RB, Bour LJ, Hilgevoord AA, Speelman JD, Ongerboer de Visser BW, 1995. Soleus H-reflex tests in dystonia. Mov. Disord 10, 44–50. 10.1002/mds.870100109. [PubMed: 7885355]

Kumru H, Albu S, Valls-Sole J, Murillo N, Tormos JM, Vidal J, 2015. Influence of spinal cord lesion level and severity on H-reflex excitability and recovery curve. Muscle Nerve 52, 616–622. 10.1002/mus.24579. [PubMed: 25600844]

Lin J-P, Lumsden DE, Gimeno H, Kaminska M, 2014. The impact and prognosis for dystonia in childhood including dystonic cerebral palsy: a clinical and demographic tertiary cohort study. J. Neurol. Neurosurg. Psychiatry 85, 1239–1244. 10.1136/jnnp-2013-307041. [PubMed: 24591458]

McCulloch PR, Milne B, 1990. Neurological phenomena during emergence from enflurane or isoflurane anaesthesia. Can. J. Anaesth 37, 739–742. 10.1007/BF03006531. [PubMed: 2225290]

Nijmeijer SWR, de Bruijn E, Forbes PA, Kamphuis DJ, Happee R, Koelman JHTM, Tijssen MAJ, 2014. EMG coherence and spectral analysis in cervical dystonia: discriminative tools to identify dystonic muscles? J. Neurol. Sci 347, 167–173. 10.1016/j.jns.2014.09.041. [PubMed: 25305713]

Oleas J, Yokoi F, DeAndrade MP, Pisani A, Li Y, 2013. Engineering animal models of dystonia. Mov. Disord 28, 990–1000. 10.1002/mds.25583. [PubMed: 23893455]

Pizzi A, Carlucci G, Falsini C, Verdesca S, Grippo A, 2005. Evaluation of upper-limb spasticity after stroke: a clinical and neurophysiologic study. Arch. Phys. Med. Rehabil 86, 410–415. 10.1016/j.apmr.2004.10.022. [PubMed: 15759220]

Rice J, Skuza P, Baker F, Russo R, Fehlings D, 2017. Identification and measurement of dystonia in cerebral palsy. Dev. Med. Child Neurol 59, 1249–1255. 10.1111/dmcn.13502. [PubMed: 28786476]

Rosenberg H, Clofine R, Bialik O, 1981. Neurologic changes during awakening from anesthesia. Anesthesiology 54, 125–130. [PubMed: 7469090]

Rumajogee P, Bregman T, Miller SP, Yager JY, Fehlings MG, 2016. Rodent hypoxia–ischemia models for cerebral palsy research: a systematic review. Front. Neurol 7, 57. 10.3389/fneur.2016.00057. [PubMed: 27199883]

Ryu Y, Ogata T, Nagao M, Kitamura T, Morioka K, Ichihara Y, Doi T, Sawada Y, Akai M, Nishimura R, Fujita N, 2017. The swimming test is effective for evaluating spasticity after contusive spinal cord injury. PLoS One 12, e0171937. 10.1371/journal.pone.0171937. [PubMed: 28182676]

Sanger TD, Ferman D, 2017. Similarity of involuntary postures between different children with dystonia. Mov. Disord. Clin. Pract 4, 870–874. 10.1002/mdc3.12533. [PubMed: 30868098]

Sanger TD, Chen D, Fehlings DL, Hallett M, Lang AE, Mink JW, Singer HS, Alter K, Ben-Pazi H, Butler EE, Chen R, Collins A, Dayanidhi S, Forssberg H, Fowler E, Gilbert DL, Gorman SL, Gormley ME, Jinnah HA, Kornblau B, Krosschell KJ, Lehman RK, MacKinnon C, Malanga CJ, Mesterman R, Michaels MB, Pearson TS, Rose J, Russman BS, Sternad D, Swoboda KJ, Valero-Cuevas F, 2010. Definition and classification of hyperkinetic movements in childhood. Mov. Disord 25, 1538–1549. 10.1002/mds.23088. [PubMed: 20589866]

Schneider SA, Edwards MJ, Grill SE, Goldstein S, Kanchana S, Quinn NP, Bhatia KP, Hallett M, Reich SG, 2006. Adult-onset primary lower limb dystonia. Mov. Disord 21, 767–771. 10.1002/mds.20794. [PubMed: 16456826]

SCPE, 2002. Prevalence and characteristics of children with cerebral palsy in Europe. Dev. Med. Child Neurol 44, 633–640. [PubMed: 12227618]

Shakkottai VG, Batla A, Bhatia K, Dauer WT, Dresel C, Niethammer M, Eidelberg D, Raike RS, Smith Y, Jinnah HA, Hess EJ, Meunier S, Hallett M, Fremont R, Khodakhah K, LeDoux MS, Popa T, Gallea C, Lehericy S, Bostan AC, Strick PL, 2017. Current opinions and areas of consensus on the role of the cerebellum in dystonia. Cerebellum 16, 577–594. 10.1007/s12311-016-0825-6. [PubMed: 27734238]

Sharma J, Johnston MV, Hossain M, 2014. Sex differences in mitochondrial biogenesis determine neuronal death and survival in response to oxygen glucose de-privation and reoxygenation. BMC Neurosci. 15, 9. 10.1186/1471-2202-15-9. [PubMed: 24410996]

Sun H, Juul HM, Jensen FE, 2016. Models of hypoxia and ischemia-induced seizures. J. Neurosci. Methods 260, 252–260. 10.1016/j.jneumeth.2015.09.023. [PubMed: 26434705]

Tekgül H, Polat M, Tosun A, Serdaroğlu G, Gökben S, 2013. Electrophysiologic assessment of spasticity in children using H-reflex. Turk. J. Pediatr 55, 519–523. [PubMed: 24382533]

Tijssen MAJ, Münchau A, Marsden JF, Lees A, Bhatia KP, Brown P, 2002. Descending control of muscles in patients with cervical dystonia. Mov. Disord 17, 493–500. 10.1002/mds.10121. [PubMed: 12112196]

Westbom L, Hagglund G, Nordmark E, 2007. Cerebral palsy in a total population of 4–11 year olds in southern Sweden. Prevalence and distribution according to different CP classification systems. BMC Pediatr. 7, 41. 10.1186/1471-2431-7-41. [PubMed: 18053264]

Wood T, Hobbs C, Falck M, Brun AC, Løberg EM, Thoresen M, 2017. Rectal temperature in the first five hours after hypoxia–ischemia critically affects neuropathological outcomes in neonatal rats. Pediatr. Res 83, 536–544. 10.1038/pr.2017.51. [PubMed: 28288145]

Yates C, Charlesworth A, Allen SR, Reese NB, Skinner RD, Garcia-Rill E, 2008. The onset of hyperreflexia in the rat following complete spinal cord transection. Spinal Cord 46, 798–803. 10.1038/sc.2008.49. [PubMed: 18542097]

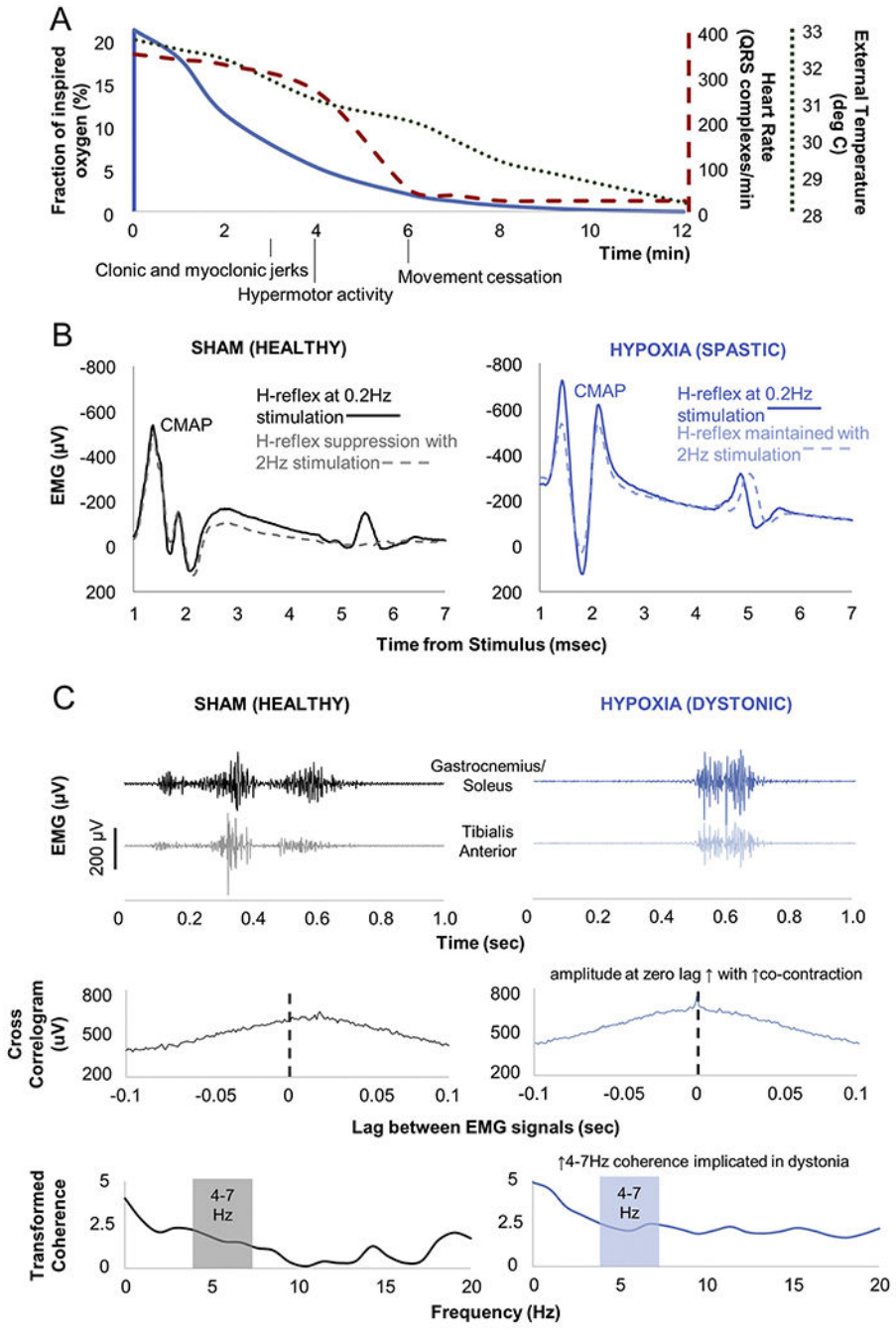

Fig. 1.

Overview of hypoxia exposure and motor electrophysiologic assessments. A) Vital sign and motor changes during neonatal hypoxia exposure. Axes and the vital signs to which they correspond have comparably coded lines. Vital signs did not vary significantly between pups during hypoxia exposure. B) Example Hoffman (H) reflexes. H-reflexes are analogues of the spinal stretch reflex that emerge following compound muscle action potentials (CMAP). H-reflexes normally suppress with high frequency stimulation (sham animal), but do not suppress with upper motor neuron injury (hypoxia-exposed animal).

C) Example dystonia measures. Electromyography (EMG) during restrained isometric voluntary hindlimb contraction shows antagonist muscle co-contraction in the sham-exposed animal, but greater co-contraction in the hypoxia-exposed animal. Cross-correlogram measures EMG signal correlation across time. Transformed coherence measures oscillatory synchrony between signals. EMG signals have been rectified and leveled to remove amplitude information. Cross-correlogram and coherence distributions have been normalized using the Fisher z-transform.

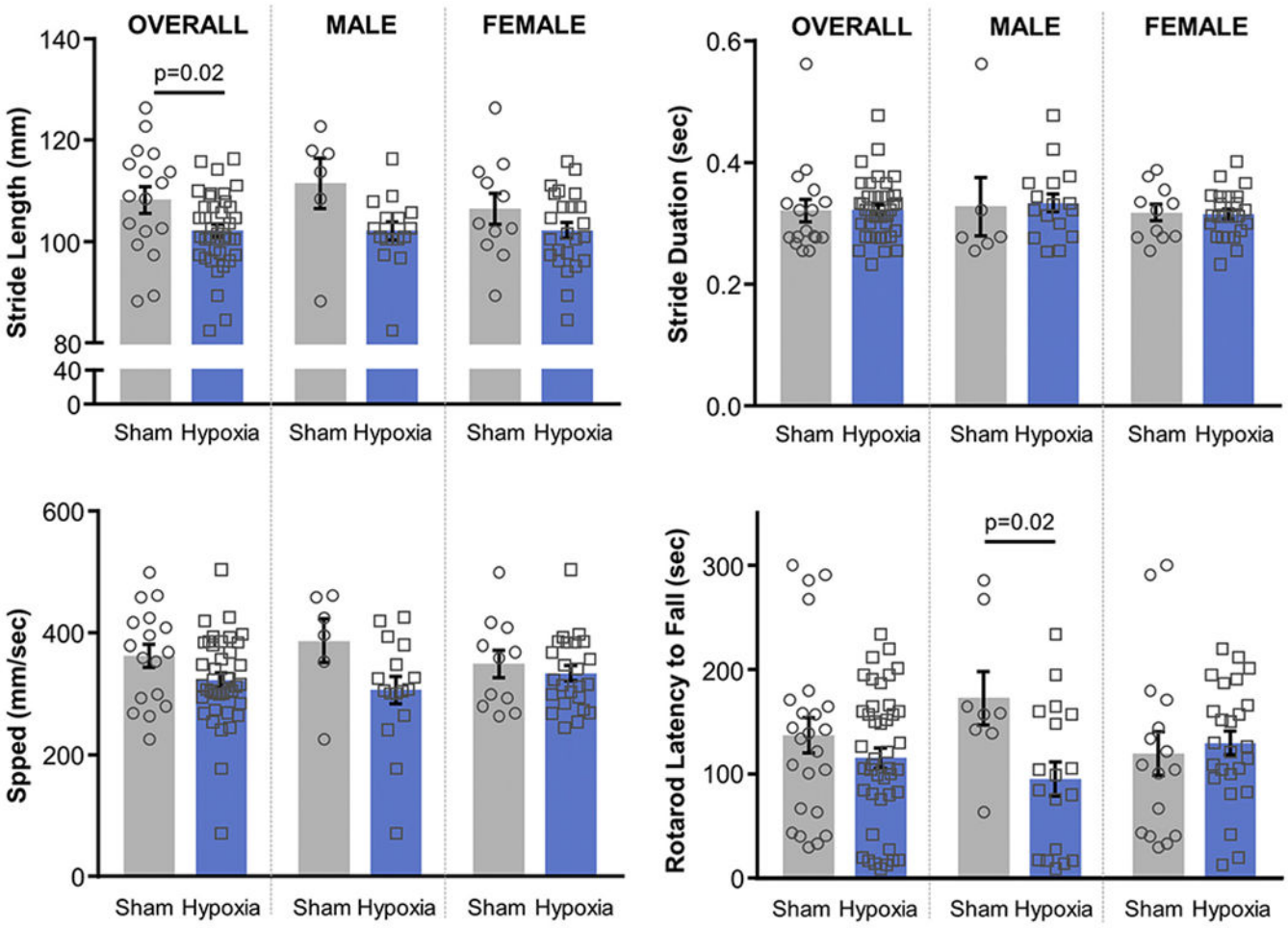

Fig. 2.

Functional motor measures. Stride length, stride duration, and speed were determined from video gait analysis. Rotarod latency to fall was measured during acceleration from 4 to 40 revolutions/min over 5 min. *P*-values < .05 indicated (MANOVA with post-hoc Tukey HSD, Table 1).

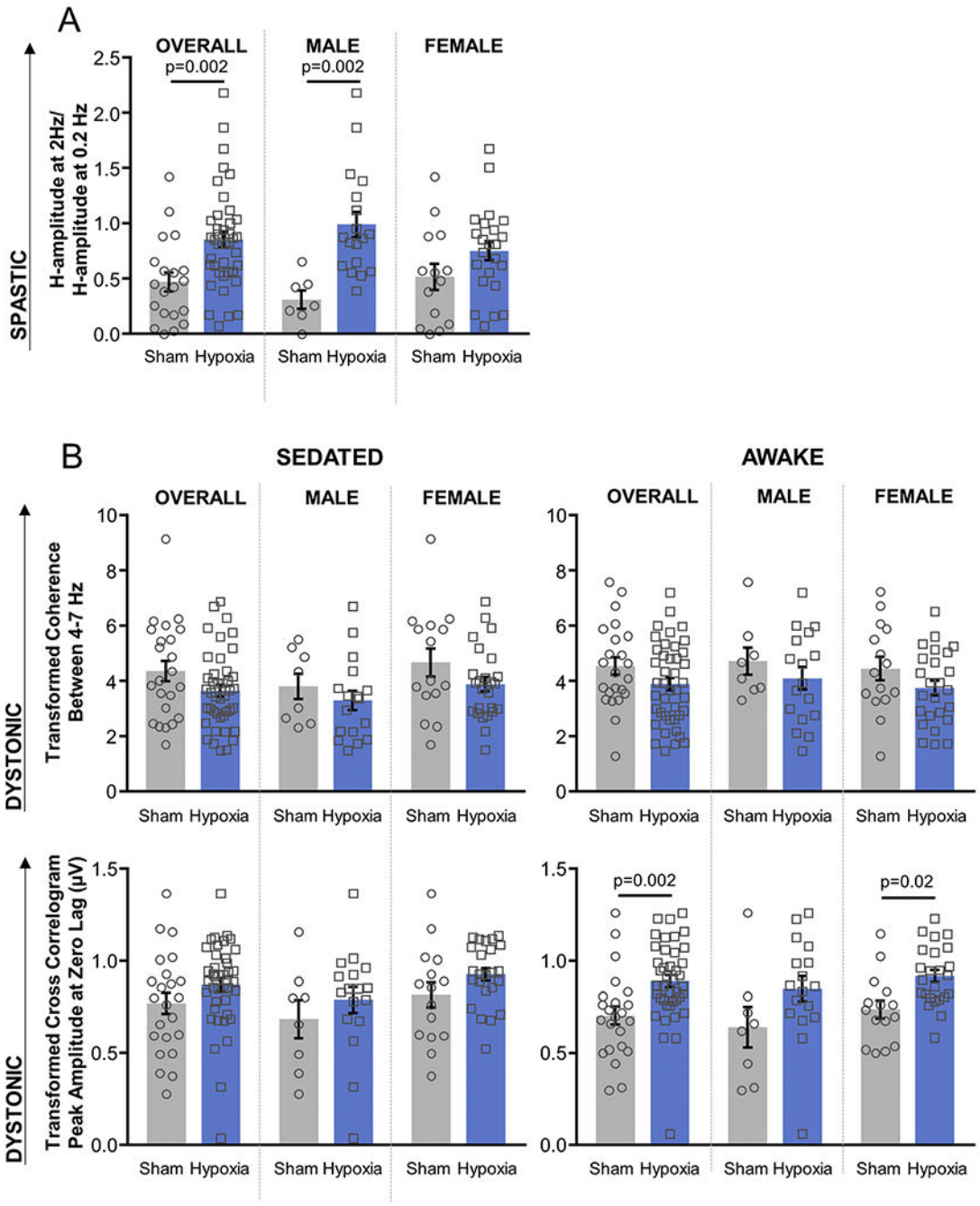

Fig. 3.

Electrophysiologic motor measures. A) H-reflex suppression (spasticity analogue, Fig. 1B); B) Transformed coherence between 4 and 7 Hz and transformed cross-correlogram amplitude at zero lag (dystonia analogues, Fig. 1C). EMG signals have been rectified and leveled to remove amplitude information. Cross-correlogram and coherence distributions have been normalized using the Fisher z-transform. P-values < .05 indicated (MANOVA with post-hoc Tukey HSD, Table 1).

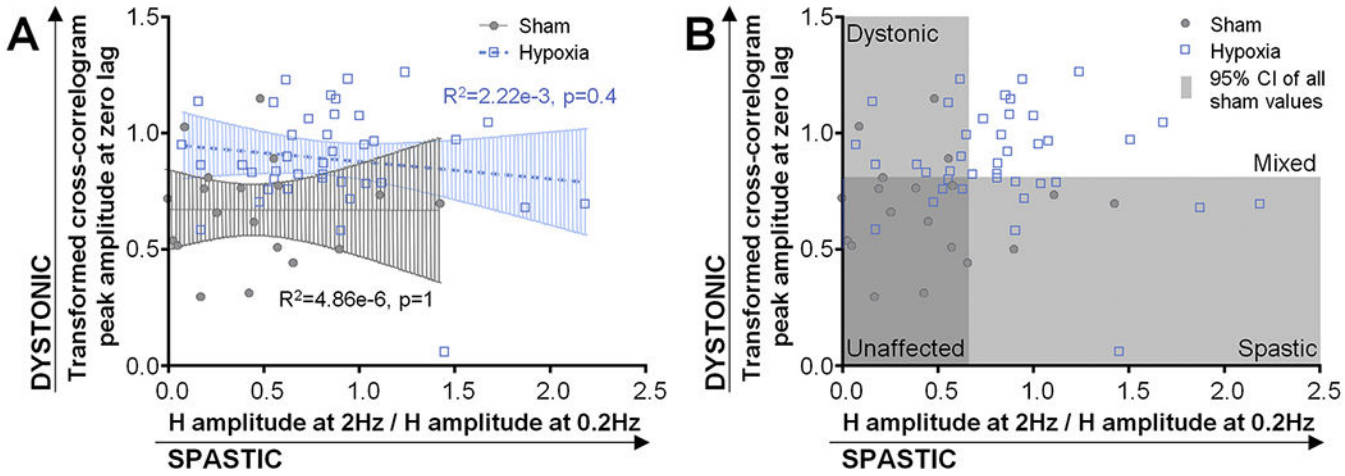

Fig. 4.

Relationship between cross-correlogram amplitude and H-reflex suppression in sham and hypoxia-exposed animals. Pearson correlation R^2 and *p*-values indicated.

Table 1

Functional and electrophysiologic motor measures separated by sex.

Motor measures	Overall			Male			Female		
	Sham	**Hypoxia**	***p***	**Sham**	**Hypoxia**	***p***	**Sham**	**Hypoxia**	***p***
	***n* = 24**	***n* = 43**		***n* = 8**	***n* = 18**		***n* = 16**	***n* = 25**	
Rotarod latency to fall (sec)	104–170, n = 24	95.8–134, n = 43	0.2	**123–222, n = 8**	**63–127, n = 18**	**0.02**	74.6–164, n = 16	106–153, n = 25	1.0
Stride length (mm)	**103–113, *n* = 17**	**99.9–104, *n* = 40**	**0.02**	101–121, *n* = 6	98.6–106, n = 16	0.1	99.6–113, *n* = 11	99.0–105, n = 24	0.2
Stride duration (sec)	0.286–0.357, n = 17	0.308–0.338, n = 40	0.9	0.234–0.422, n = 6	0.305–0.363, n = 16	1.0	0.288–0.348, n = 11	0.299–0.332, n = 24	1.0
Speed (mm/s)	325–400, n = 17	300–346, n = 40	0.07	316–458, n = 6	262–350, n = 16	0.1	299–400, n = 11	309–359, n = 24	0.8
H-reflex suppression	**0.303–0.637, *n* = 20**	**0.717–0.992, *n* = 41**	**0.002**	**0.150–0.470, *n* = 7**	**0.766–1.21, n = 18**	**0.002**	0.264–0.769, *n* = 13	0.576–0.924, *n* = 23	0.2
Coherence - sedate	3.63–5.09, n = 23	3.22–4.06, *n* = 42	0.08	2.88–4.71, n = 8	2.59–3.99, n = 17	1.0	3.58-5.75, *n* = 15	3.34–4.42, n = 25	0.08
Coherence - awake	3.92–5.16, n = 23	3.44–4.33, n = 42	0.1	3.75–5.67, n = 8	3.31–4.89, n = 17	0.6	3.54–5.35, n = 15	3.19–4.29, n = 25	0.6
Cross-correlation – sedate	0.657–0.882, n = 23	0.798–0.942, n = 42	0.1	0.483–0.883, n = 8	0.649–0.927, n = 17	0.6	0.667–0.963, n = 15	0.857–0.999, n = 25	0.6
Cross-correlation - awake	**0.605–0.798, n = 43**	**0.822–0.956, n = 42**	**0.002**	0.422–0.856, n = 8	0.714–0.982, n = 17	0.08	**0.631–0.840, n = 15**	**0.850–0.986, n = 25**	**0.02**

95% confidence intervals based on the normal distribution and animal numbers for each group are shown. Comparisons are via MANOVA with post-hoc Tukey HSD comparing sham and hypoxia-exposed animals within each group. For Hoffman (H) reflex suppression, 0 indicates complete H-reflex suppression and 1 indicates no suppression, as would be seen in spasticity. Comparisons with $p < .05$ are in bold.